J Solid State Electrochem (2011) 15:2409–2417
DOI 10.1007/s10008-011-1445-1

ORIGINAL PAPER

Influence of silanization on voltammetry at electrodes modified with silica films of controlled porosity formed by electrochemically initiated sol-gel processing

James A. Cox · Kamila M. Wiaderek · B. Layla Mehdi · Benjamin P. Gudorf · David Ranganathan · Silvia Zamponi · Mario Berrettoni

Received: 24 March 2011 / Revised: 30 April 2011 / Accepted: 2 May 2011 / Published online: 18 June 2011

Abstract Silica sol-gel (SG) films with templated pores were deposited on glassy carbon (GC) electrodes by an electrochemically initiated process. Generation-4 poly(amidoamine), PAMAM, dendrimer was included in the tetraethoxysilane precursor to facilitate pore formation. The PAMAM adsorbs to the GC, which blocks SG formation at those sites on the electrode. The pore size was 10±5 nm. After removal of the PAMAM, cyclic voltammetry of $Fe(CN)_6^{3-}$ and $Ru(NH_3)_6^{3+}$ at pH 6.2 showed that the residual negative charge on the silica attenuated the current for the former and increased the current for the latter, presumably by electrostatic repulsion and ion-exchange preconcentration, respectively. This premise was supported by repeating the measurements at the isoelectric point. Methylation of the silanol sites was used to eliminate the charge of the SG. At the end-capped SG, the voltammetry of $Fe(CN)_6^{3-}$ and $Ru(NH_3)_6^{3+}$ yielded currents that were independent of pH over the range 2.1 to 7.2. Circumventing the need for the silanization by using (3-glycidyloxypropyl)trimethoxysilane as the sol-gel precursor failed because the oxygen plasma treatment to remove the PAMAM attacked the organically modified sol-gel backbone. The resulting modified electrode mitigated the influence of proteins on the voltammetry of test species and stabilized functionalize nanoparticle catalysts under hydrodynamic conditions.

Keywords Sol-gel · Silanize · Pore structure · Voltammetry · Isoelectric point

Dedicated to Prof. George Inzelt on the occasion of his 65th birthday.

J. A. Cox (✉) · K. M. Wiaderek · B. L. Mehdi · B. P. Gudorf
Department of Chemistry and Biochemistry, Miami University, Oxford, OH 45056, USA
e-mail: coxja@muohio.edu

D. Ranganathan · S. Zamponi
Department of Chemical Science, University of Camerino, Via S. Agostino 1, 62032 Camerino, Italy

M. Berrettoni
Department of Physical and Inorganic Chemistry, University of Bologna and Unità di Ricerca, INSTM di Bologna, Viale Risorgimento 4, 40136 Bologna, Italy

Introduction

Contamination of electrode surfaces by adsorption of matrix components and/or analytes complicates electroanalytical methodology by compromising repeatability of measurements. In extreme cases, adsorption precludes these measurements by passivating the electrode. An approach to alleviating interference from matrix components is to coat the electrode with a film of controlled porosity. In this case, the pores must be larger than the diameter of the analyte but smaller than the size of potential interferents. To our knowledge, the first application of such a film was by Sittampalam and Wilson [1] who used cellulose acetate (CA) as a coating on a platinum electrode to facilitate the electrochemical detection of hydrogen peroxide in the presence of bovine serum albumin (BSA) and other proteins. The negative charge on the CA also mitigated the interference of ascorbate on the determination of hydrogen peroxide [1, 2]. The size-exclusion property of CA was used along with incorporation of a catalyst, cobalt phthalocyanine (CoPC), in the design of an electrochemical detector for application to flow systems [3]. Base hydrolysis was used to control the pore size of CA.

Sol-gel films have potential advantages over organic materials such as CA as electrode modifiers. Resulting matrices such as silica are chemically and physically robust, capable of hosting catalysts in the bulk material [4] and/or in pores, and amenable to control of the film structure. They share with CA the property of having a negative charge over a wide pH range. This charge can impart selectivity of voltammetric measurements by Donnan exclusion of anions in a liquid sample [1, 2]; however, it can be detrimental to a wide range of voltammetric applications of such film-modified electrodes. Whereas the size of the pores in CA can be varied by hydrolysis, a single approach is not available for sol-gel processing. Templating pores in sol-gel materials by adding surfactants to the precursor is a well-established method, particularly for obtaining pores in the 2–5 nm range [5]. Macroporous silica films (pore diameters greater than 50 nm) were obtained by spin-coating an electrode in TMOS that contained polystyrene spheres which were subsequently dissolved [6, 7]. A general goal of our program is to fabricate a sol-gel film on an electrode that is neutral over a wide pH range and contains non-tortuous pores of a controlled size in the 5–50 nm range that directly link a liquid sample to the electrode surface. This size range is significant in applications of voltammetry to study of biological samples and potentially important to applications of nanoparticle-modified electrodes.

Casting and spin-coating are perhaps the most widely used means of forming sol-gel films on electrodes, but in this study, electrochemically initiated deposition, which was introduced by Mandler and coworkers [8–10], was employed. This approach to film formation provides a convenient way to control film thickness in the range <100 nm. In the initial report [8], a two-step process was used with a methyltrimethoxysilane (MeTMOS) precursor. First, in bulk solution, MeTMOS was partially hydrolyzed to form $MeSi(OH)_3$ in the liquid phase. Next, the $MeSi(OH)_3$ at the electrode surface was converted to a sol-gel film by a hydroxide-catalyzed reaction. The hydroxide was produced by reduction of water, proton, and/or supporting electrolyte in the unbuffered medium. By selection of the potential, the rate of hydroxide production was controlled, which, in turn, was a factor in determining the thickness of the sol-gel layer. The method was extended to other combinations of electrodes and precursors, including tetraethoxysilane (TEOS) [11] and tetramethoxysilane (TMOS) [12].

Walcarius et al. [13] developed an analogous method that yielded sol-gel films with vertically aligned pores on electrodes. Application of a cathodic potential to an electrode in contact with a pH 3 surfactant, cetyltrimethylammonium (CTAB), and hydrolyzed TEOS, organized CTAB at the surface and generated hydroxide ion, which catalyzed sol-gel formation on the electrode. In combination, these phenomena yielded a film with CTAB-templated pores vertical to the electrode surface. The film thickness grew at about 8 nm s^{-1} for the first 30 s. This general method, but with selected ratios of MeTMOS and TEOS in the sol, yielded films with a varying degree of methylation [14]. The films with greater degrees of methylation suppressed the voltammetric current for the oxidation of $Ru(bpy)_3^{2+}$ by either a hydrophobic effect or by a decreased pore volume that resulted from pendant methyl groups. Similar but non-methylated films were prepared by evaporation-induced self assembly in which dip-coating electrodes in aged sols formed from mixtures CTAB and TEOS was employed [15]. Cyclic voltammetry of ferrocene methanol (FcMeOH), $Ru(bpy)_3^{2+}$ and $Fe(CN)_6^{3-}$ at pH 4.1 was characterized by an influence of the negative sites of silica on the mass transport through this film, which had ca. 2-nm pores. That is, evidence of exchange of $Ru(bpy)_3^{2+,3+}$ and of $FcMeOH^+$ onto the sol-gel film was obtained, and a suppression of the peak currents for the $Fe(CN)_6^{3-,4-}$ couple was observed. This influence of residual charge on mass transport is consistent with a previous result where spin-coated sol-gel films on electrodes were processed to contain amine or acetate functionalities [16].

In the present study, our objective was to coat electrodes with sol-gel films that had the size-exclusion capability of cellulose acetate [1, 2] but with more amenability to further chemical modification. The targeted structure was a dense (microporous) sol-gel film of controlled thickness through which pores that provided a direct (non-tortuous) path between liquid samples and the electrode surface were present. The sol-gel was deposited by an acid-catalyzed, electrochemically assisted process [8–10]. Based on our previous work [17], inclusion of generation-4 poly(amidoamine) dendrimer (PAMAM) in the precursor solution resulted in the formation of pores. Our hypothesis is that generation of the proton catalyst is blocked at sites on the electrode that are covered by adsorbed PAMAM, so sol-gel processing does not occur at these points. The result is the formation of a pore (void volume) in the film above these sites of adsorption. The PAMAM is removed prior to electrochemical application of the modified electrode. Because generations 4–10 PAMAM adsorb to various substrates in a manner that yields homogeneous patterns [18, 19] and the diameter these adsorbed moieties varies with the generation number [19], this approach can potentially provide a means of controlling pore size over a wide range. In general, a proof of this concept that an adsorbed species on the surface of an electrode that is being coated by electrochemically assisted sol-gel processing can provide a route to control of pore size in the film, thereby complementing procedures that use a templating agent. Finally, capping negative sites on the silica sol-gel with methyl groups was explored as a means of addressing the

perturbation of the voltammetry of ions by their interaction with exchange sites on the pore walls. The resulting modified electrode was applied to measurements in protein-containing media and as an amperometric detector in a flow cell.

Experimental

Reagents and apparatus

Potassium ferricyanide, potassium chloride, sodium formate, formic acid, and methanol, which were ACS Reagent Grade, were from Fisher Scientific (Fair Lawn, NJ). Tetraethoxysilane (TEOS) at 99+% purity, lithium perchlorate, trichloromethylsilane, trimethylchlorosilane, ruthenium hexamine, dichloromethane, acetonitrile, ferrocene, and carbon tetrachloride were obtained from Aldrich (Milwaukee, WI). The 2-propanol (99.5%) was from Alfa Aesar (Ward Hill, MA). All chemicals were used as received except that the carbon tetrachloride was redistilled (note: toluene can be substituted for the CCl_4). Bovine serum albumin (BSA), 98% purity, and phosphatidylcholine, 99%, were obtained from Sigma-Aldrich (St. Louis, MO). Water used in this study was house-distilled that was further purified with a Barnstead NANO pure II system.

The electrochemical experiments were performed with CH Instruments (Austin, TX) Models 400, 660B, and 800 electrochemical workstations. Generally, the working electrode was a 3.0-mm diameter glassy carbon (GC) that was polished with 0.05 μm alumina and rinsed with distilled water in an ultrasonic bath before each experimental sequence. In some cases, the working electrode was indium tin oxide (ITO) that was purchased from Delta Technologies, Limited (Stillwater, MN). The ITO was rinsed with ethanol, dried under nitrogen, and cut into squares with 1.5-cm edges prior to use as an electrode. Using a rubber o-ring, a 0.32-cm^2 portion of the ITO was isolated as the working electrode. Unless otherwise noted, all potentials were measured and reported versus an Ag|AgCl, 3 M KCl reference electrode from Bioanalytical Systems (West Lafayette, IN). Platinum gauze was the counter electrode. The solutions were deaerated with nitrogen gas when the experiments involved a potential excursion that was negative of 0.0 V.

Infrared spectra were obtained in the ATR mode, using a Perkin Elmer Spectrum 100 Series FT-IR spectrometer (Shelton, CT). Scanning electron microscopy (SEM) images were obtained on a Zeiss Supra 35VP FEG microscope (Oberkochen, Germany). The pore size determination used Image-Pro® Plus software. The gas plasma was generated with a device obtained from March Plasma Systems (Concord, CA). The system was operated at 100 W and 0.3 Torr [20].

Formation of the silica sol-gel films

The general electrochemically initiated deposition process was adapted from Mandler and coworkers [8–10] with the formation of the pores based on our previous report [17]. The precursor solution consisted of 5 mL of 0.1 M lithium perchlorate in 2-propanol, 2.5 mL of H_2O, and 175 μL of G4-PAMAM. The pH of the solution was adjusted to 4.0 with dilute HCl, after which 2.5 mL of TEOS was added. The electrode was immersed in the freshly prepared solution. After 30 min, 1.5 V vs. a platinum quasi-reference electrode was applied for 30 min to generate an acidic environment at the electrode-solution interface, which catalyzed formation of the sol-gel on the electrode surface. During this deposition process, the solution was quiescent. Under controlled potential conditions, the electrode was withdrawn from the solution at a constant rate of 0.5 mm min^{-1}. Residual solution was removed, after which the electrodes were air-dried and aged overnight under ambient conditions in a vessel that was covered with punctured Parafilm. A control experiment was performed as above except the electrode was at open circuit; cyclic voltammetry of 1.0 mM $Ru(NH_3)_6^{3+}$ in 0.1 M KCl at pH 4.0 gave a cathodic peak current that was within 5% of that at a bare ITO of the same area under the same conditions, demonstrating that no sol-gel is deposited under this condition.

Unless otherwise noted, prior to use, PAMAM was removed from the silica film with an oxygen plasma [17, 20, 21]. We previously demonstrated that exposing the film to the activated oxygen gas for 20 min is sufficient for complete removal of the PAMAM [17]. When glassy carbon is used, the resulting nanoporous sol-gel coated electrode is designated herein as GC|npSG.

The procedure for end-capping the GC|npSG was based on a silanization method reported by Evans et al. [22].The GC|npSG was treated with 1.0 mM trichloromethylsilane in CCl_4 at room temperature for 120 min, which was followed by washing with CCl_4 to remove un-reacted silane. Next, the film was reacted with dry methanol for 120 min to convert the residual chlorine sites to methoxy groups. The film was rinsed with dichloromethane and dried overnight as described above. Finally, the film was treated for 120 min at room temperature with 1.0 mM trimethylchlorosilane in CCl_4, rinsed with dichloromethane, and dried overnight. The resulting end-capped system was designated as GC|npSG-EC.

Results and discussion

Initial experiments were performed with electrodes modified as described in the Experimental section except that the

sol-gel was deposited from precursors in both the presence and absence of the PAMAM. Cyclic voltammetry was performed on 0.5 mM $Fe(CN)_6^{3}$ in 0.1 M KCl at a scan rate, v, of 50 mV s^{-1}. The reduction of $Fe(CN)_6^{3-}$ was not observed when the sol-gel was deposited at 1.5 V by an acid-catalyzed process in the absence of PAMAM. A report of an analogous experiment with base-catalyzed processing (−1.1 V applied for 30 min) of an ormosil film yielded a marginally observable peak for the reduction of $Fe(CN)_6^{3-}$ [8]. The complete blocking of the reduction in the present study is likely occurred because acid-catalyzed sol-gel processing yields a denser material than that obtained by base-catalyzed processing. Moreover, organic sites on the silica in the previously reported study [8] can increase the porosity relative to that of an otherwise identical purely inorganic material [23].

When the film was deposited in the presence of PAMAM, a cyclic voltammogram for 1.0 mM $Fe(CN)_6^{3-}$ in 0.1 M KCl was observed, which is evidence that inclusion of PAMAM in the precursor solution causes the formation of pores. Figure 1 shows a model of a hypothesis for the pore formation in the presence of PAMAM. The hypothesis is based on the known adsorption of PAMAM on surfaces [18, 19]. The adsorbed PAMAM is proposed to block hydronium generation, which restricts growth of the film to zones above the bare electrode. The result is pores in the sol-gel film that are above the sites of adsorbed PAMAM. Data presented below provide support for this model, but it cannot be precluded that some voids in the sol-gel from PAMAM encapsulated therein will also be present. An SEM image obtained after the oxygen plasma treatment suggested that the sol-gel structure was not damaged and that the pore diameters were in the range of 10±5 nm (Fig. 2). The lack of damage supports the hypothesized model in that decomposition of any encapsulated PAMAM by the plasma is likely to cause damage to the surrounding sol-gel. The pore size is greater than the calculated diameter of generation-4 poly(amidoamine), 4.5 nm; however, it is in the expected range given that clustering and deformation upon adsorption of PAMAM occur [18, 19]. The film thicknesses were measured by SEM and AFM at an edge formed by peeling the deposit from the substrate. Values obtained were in the range of 70–100 nm.

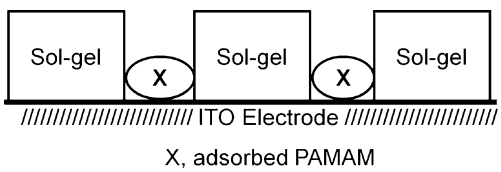

Fig. 1 Model of the formation of pores in a sol-gel formed by electrochemically assisted processing in the presence of PAMAM

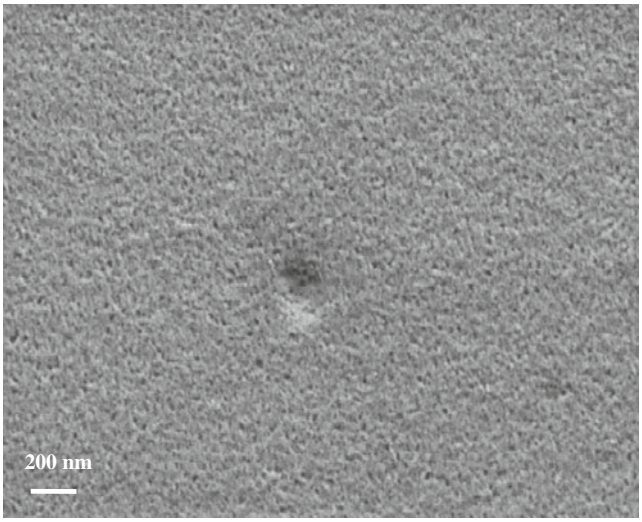

Fig. 2 Scanning electron microscopy of GC|npSG

To verify that the oxygen plasma treatment does not alter the sol-gel structure, cyclic voltammetry of ferrocene (Fc) in acetonitrile was performed at GC|npSG before and after removal of the PAMAM (Fig. 3). A 3% increase in peak current was observed upon removal of the PAMAM. If structural damage such as the formation of cracks in the sol-gel had occurred, a large increase is peak current will have been observed because of increased exposure of the GC to the liquid phase. The 3% increase is probably related to more direct contact between the GC surface and the Fc after the PAMAM was removed. In addition, the voltammetry was performed at the GC electrode prior to deposition of the SG film. From the currents at GC and GC|npSG, 40% of the surface is blocked by the SG matrix. The oxidation of Fc at GC|npSG after removal of the PAMAM gave a current limited by semi-infinite linear diffusion. In this regard, under the conditions in Fig. 3, the slope of a plot of log i_{pa} vs. log v (i_{pa}, anodic peak current; v, scan rate) where v was varied over the range 20–250 mV s^{-1} was 0.47, which is comparable to the theoretical value of 0.50.

The selection of the neutral species, Fc, in the above experiment was to preclude perturbation of the voltammetry of ionic species by the surface charge of silica. In this regard, voltammetry of ionic species at electrodes modified with films containing ion-exchange sites, including mesoporous silica, is markedly influenced by the repulsion of co-ions and attraction of counter-ions [15, 16, 23–25]. Silica sol-gels contain silanol groups that are de-protonated at pH values above ca. 2, the isoelectric point [7, 15, 26], thereby producing a negatively charged surface. A predicted result is that the influence of ion-exchange on the mass transport will be less with SGs that contain pores resulting from adsorbed PAMAM than that observed at surfactant-templated SGs because of the larger pore size and smaller pore density in the former case. To test this prediction,

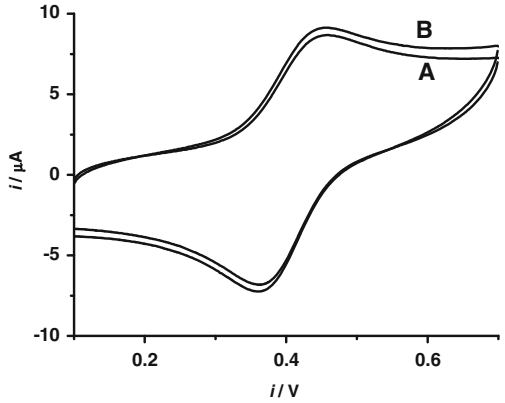

Fig. 3 Cyclic voltammetry of 0.5 mM ferrocene in acetonitrile containing a 0.5 M Bu_4NPF_6 supporting electrolyte. Electrode: GC|npSG **a** before and **b** after oxygen plasma treatment; *v*, 50 mV s^{-1}

cyclic voltammetry of 0.5 mM $Fe(CN)_6^{3-}$ was compared at GC and GC|npSG in pH 7.2 phosphate buffer (0.1 M) at 50 mV s^{-1}. At GC, the cathodic peak current, i_{pc}, was 8.2 μA, and at GC|npSG, the peak current for the reduction of $Fe(CN)_6^{3-}$ was 2.0 μA. This decrease is significantly less than that the 90% attenuation observed for the reduction of $Fe(CN)_6^{3-}$ at pH 4.1 with SG films that have closely spaced pores in the 2-nm range [15]. It should be noted, however, that because of the difference in pH, ionic strength, and film thickness, this comparison is very qualitative.

In contrast to the experiments with Fc, the voltammetry of ionic species at GC|npSG electrodes was not diffusion limited. With 0.5 mM $Fe(CN)_6^{3-}$ as the electroactive species in pH 7.2 phosphate buffer, the slope of a plot of log i_{pc} vs. log *v*, where *v* was varied over the range 20–250 mV s^{-1}, was 0.31. Common factors that can give a slope <0.50 are chemical or electrochemical kinetics and radial diffusion, which is favored by a decrease in the diameter of a disk electrode. The negative charge on the walls of the pores may restrict transport of $Fe(CN)_6^{3-}$ to a channel that is narrower than the physical size of the pore. By conversion, the scan rate to the time domain [27], the time scale of these voltammetry experiments is about 0.1–1.3 s. The diffusion distances corresponding to these times are far greater than the film thickness, so the current-limiting process is diffusion to the pore–sample interface. With closely packed pores, diffusion fields overlap to the extent that radial diffusion will not be the limiting factor. If the electrostatic effect causes a decrease in the apparent channel size through which $Fe(CN)_6^{3-}$ is transported to a degree where radial diffusion partially controls mass transport, a slope <0.50 will be observed. With 0.5 mM $Ru(NH_3)_6^{3+}$ as the electroactive species, i_{pc} at 50 mV s^{-1} was 6.8 μA with the GC|npSG electrode. Based on the results with Fc as the test species, where perturbation by ion exchange is precluded, this current is higher than the value expected, 6.2 μA. Preconcentration of $Ru(NH_3)_6^{3+}$ on the negative sites apparently is occurring but to a much lesser degree than in the case of CTAB-templated sol-gel films where the amplification factor was >10 for $Ru(bpy)_3^{2+}$ [15]. Consistent with some ion exchange of $Ru(NH_3)_6^{3+}$ onto GC|npSG at pH 7.2, the slope (0.65) of a plot of log i_{pc} vs. log *v* over the range 20–250 mV s^{-1} was >0.5; the limiting value for a surface-confined is a slope of 1.0. Ion exchange onto the sol-gel was expected; the interaction of $Cu(NH_3)_4^{2+}$ with silanol sites of a composite of carbon paste and a sol-gel has been used as the preconcentration step in the stripping voltammetry determination of that cationic complex [28].

A major goal of this study was to mitigate the influence of the surface charge on the voltammetry of ionic species at electrodes modified with a sol-gel film. It is known that controlling the pH of the supporting electrolyte into the range of the isoelectric point of silica is one such method [12, 15]. Consistent with the general trends in the previous studies, the peak currents for the reductions of $Fe(CN)_6^{3-}$ and $Ru(NH_3)_6^{3+}$ increased by 17% and decreased by 36%, respectively, when the above experiments (*v*, 50 mV s^{-1}) in pH 7.2 phosphate buffer were repeated in 0.1 M KCl adjusted to pH 2.1 with HCl. Moreover, we found that using a high ionic-strength supporting electrolyte normalizes the behavior of anions and cations in voltammetry at GC|npSG at pH values above the isoelectric point of silica. Specifically, the voltammetric behavior of $Fe(CN)_6^{3-}$ and $Ru(NH_3)_6^{3+}$ at GC|npSG was examined at various concentrations of KCl in nominally neutral solution. By comparison to investigations of the permselectivity of ion-exchange membranes as a function of ionic strength, it was hypothesized that increasing the concentration of supporting electrolyte will lead to a breakdown of the Donnan exclusion principle, resulting in the elimination of the influence of the negative sites of the silica sol-gel on the voltammetry. The results are shown in Fig. 4. Consistent with Donnan penetration of co-ions at high ionic strength, the voltammetric current for $Fe(CN)_6^{3-,4-}$ increases as the KCl concentration is increased from 0.05 to 2.0 M. The i_{pc} value in neutral 2.0 M KCl was 97% of that in 0.1 M KCl at pH 2.1 under otherwise identical conditions. Given that the precision of these measurements is about 5%, the effect of the negative sites on the sol-gel film is for all practical purposes eliminated by the use of the high ionic-strength electrolyte. It should be noted, however, that this observation is specifically for npSG where the sol-gel phase is dense (microporous) and the 10-nm pores are larger than those formed typically with a surfactant-templated, mesoporous sol-gel film on an electrode.

For applicability to a wide range of electrolytes, it is necessary to address the problem of the charged sites by modification of the sol-gel phase rather than by pH or

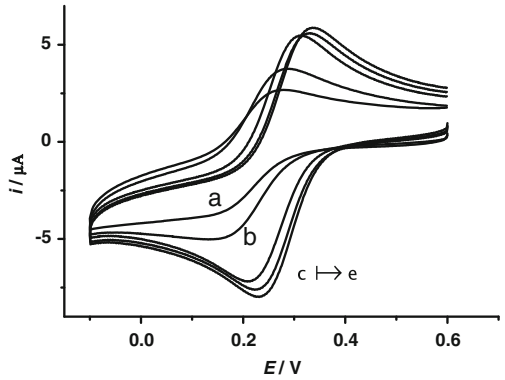

Fig. 4 Influence of ionic strength on the cyclic voltammetry of 1.0 mM $Fe(CN)_6^{3-}$ at GC|npSG in neutral solution. Supporting electrolyte, **a** 0.05 M, **b** 0.10 M, **c** 1.0 M, **d** 1.5 M, and **e** 2.0 M KCl; *v*, 50 mV s^{-1}

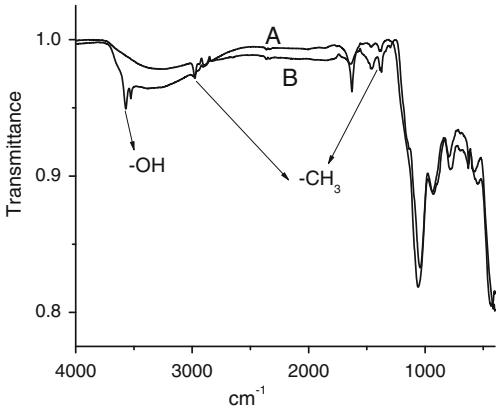

Fig. 5 Infrared spectroscopy of a TEOS-derived sol-gel film **a** before and **b** after silanization as described in the Experimental section

ionic-strength control. A potential approach is to use an organically modified precursor to form an ormosil by the electrochemically assisted deposition process [9] in conjunction with controlling pore size with an adsorbed species. In this regard, we used a previously investigated precursor, (3-glycidyloxypropyl)trimethoxysilane [29], with adsorption of PAMAM to modify the GC surface. SEM imaging after oxygen plasma treatment to remove the PAMAM illustrated that the resulting ormosil was destroyed. Our attempts to date to remove the PAMAM by a milder method such as liquid–liquid extraction have not been successful. Hence, we explored methylation of the TEOS-derived, npSG-coated electrodes as a route to eliminating the charged sites of the silica. This general procedure is used widely in the preparation of silica-based chromatographic columns. A related method, reaction of a mesoporous, TEOS-derived, sol-gel film with an aminosilane, was used previously to graft a complexing agent on the surface [30]. In the present study, the method reported by Evans et al. [22] for end-capping the silanol sites with methyl groups was employed. The efficacy of end-capping the TEOS-derived sol-gel films on GC electrodes was shown by surface infrared spectroscopy before and after the silanization described in the "Experimental" section. As shown in Fig. 5, the –OH peaks that are evident at 3,570 and 3,527 cm^{-1} on GC|npSG were diminished to below the detection limit on the end-capped film on the electrode (GC|npSG-EC). In addition, peaks at 2,878 and 2,986 cm^{-1}, which correspond to the alkyl ($-CH_3$) stretching, are observed on GC|npSG-EC. The unchanged features of the spectrum include a wide band near 3,435 cm^{-1} that corresponds to residual water, peaks at 1,630 cm^{-1} from bending of the H–O–H bonds [31], asymmetric stretching of Si–O–Si at 1,000–1,100 cm^{-1}, symmetric stretching of Si–O–Si at 799 cm^{-1}, and Si–O–Si bending at 400–500 cm^{-1}. These features are related to the general silica sol-gel structure [32–34]. The silanization procedure did not damage the sol-gel film. An SEM image obtained after this treatment was not distinguishable from that in Fig. 2. Moreover, the peak currents for the reduction of 0.5 mM ferrocene under the conditions in Fig. 3 at GC|npSG-EC agreed to within 3% with those at GC|npSG.

To determine whether methylation of the silanol alleviated the influence of the charged sites of the sol-gel on the electrode behavior, the cyclic voltammetry of $Ru(NH_3)^{3+}$ and of $Fe(CN)_6^{3-}$ pH 7.2 (Fig. 6) and pH 2.1 was studied at GC|npSG-EC. In contrast to the results at GC|npSG, i_{pc} values for these ionic test species were virtually identical (Table 1). The difference in currents is within the precision of the method and also can be related to a difference in diffusion coefficients. That the voltammetric currents were not a function of pH at GC|npSG-EC demonstrates that the end-capping procedure that was employed eliminated the negatively charged sites on the sol-gel surface. The peak currents for the reduction of $Fe(CN)_6^{3-}$ and of $Ru(NH_3)_6^{3+}$ at GC|npSG-EC at pH 7.2 were limited by semi-infinite linear diffusion in that the slopes were near the 0.50

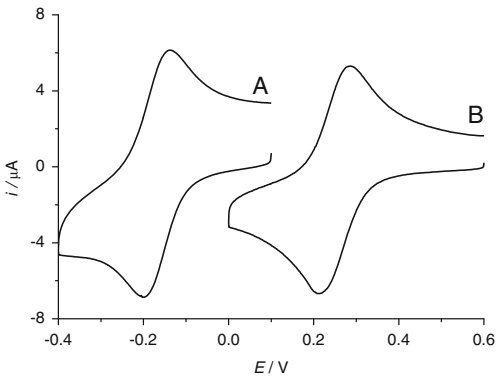

Fig. 6 Cyclic voltammetry of **a** 0.5 mM $Fe(CN)_6^{3-}$ and **b** 0.5 mM $Ru(NH_3)_6^{3+}$ at GC|npSG-EC in 0.1 M KCl at pH 6.0. *v*, 50 mV s^{-1}. At GC coated in the absence of PAMAM, reductions of $Fe(CN)_6^{3-}$ and $Ru(NH_3)_6^{3+}$ were not observed

Table 1 Cyclic voltammetry of $Ru(NH_3)^{3+}$ and of $Fe(CN)_6^{3-}$ at a GC|npSG-EC electrode as a function of pH and scan rate

Test species *C*, 0.5 mM	pH	i_{pc}, μA	log i_{pc} vs. log v[a] slope[b] (R^2)
$Ru(NH_3)_6^{3+}$	2.1	5.89	0.52 (0.999)
$Ru(NH_3)_6^{3+}$	7.2	5.94	
$Fe(CN)_6^{3-}$	2.1	5.95	0.48 (0.999)
$Fe(CN)_6^{3-}$	7.2	6.00	

At GC coated in the absence of PAMAM, reductions of $Ru(NH_3)_6^{3+}$ and $Fe(CN)_6^{3-}$ were not observed

[a] Scan rate range, 20–250 mV s^{-1}

[b] Theoretical value: semi-infinite linear diffusion, 0.50

theoretical value (Table 1). Linear diffusion control of the current at GC|npSG-EC is consistent with the above-proposed models of mass transport in the voltammetry of $Fe(CN)_6^{3-}$ and $Ru(NH_3)_6^{3+}$ at GC|npSG where departure of the slope of log i_{pc} vs. log v from 0.50 was related to residual negative charge on the sol-gel surface. Also consistent with a linear-diffusion limit at GC|npSG-EC, i_{pc} was directly proportional to concentration of ionic test species over the range of 0.5–2.5 mM. The r^2 values with $Fe(CN)_6^{3-}$ and $Ru(NH_3)_6^{3+}$ as the analytes were 0.999 and 0.998, respectively. The currents were reproducible during consecutive trials and after storage of the modified electrodes. Ten replicate trials on 0.5 mM $Fe(CN)_6^{3-}$ and 0.5 mM $Ru(NH_3)_6^{3+}$ gave standard deviations of 0.5% and 0.2%, respectively. The electrodes gave statistically identical peak currents over a 3-week period when rinsed with water and stored in a dry state in a covered, air-filled container. During this period, the electrode was used several times. Longer term stability was not investigated.

The second goal of this study was to form pores in the neutral sol-gel that were large enough for facile diffusion of analytes to the electrode surface but in a range that prevents incursion of macromolecules such as proteins. That the 10-nm pores in the present study fall in this range was illustrated by investigating the influence of adsorption of a macromolecule on the voltammetry of selected species at GC|npSG-EC. Cyclic voltammetry of $Fe(CN)_6^{3-}$ in pH 7.2 phosphate buffer was performed in the presence and

Table 2 Influence of BSA on the current for the reduction of 0.5 mM $Fe(CN)_6^{3-}$

Electrode	i_{pc}, BSA absent/μA	i_{pc}, 0.2% BSA/μA
GC	6.5	4.6
GC|npSG	4.0	2.6
GC|npSG-EC	4.3	4.2

Conditions: v, 50 mV s^{-1}; supporting electrolyte, pH 7.2 phosphate buffer; data obtained 5 min after introduction of the electrode

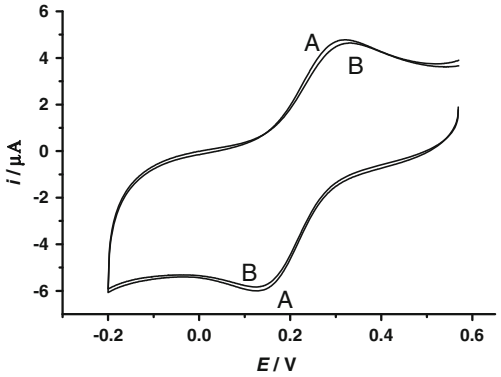

Fig. 7 Cyclic voltammetry of 1.0 mM $Fe(CN)_6^{3-}$ in the presence of 0.5 mM phosphatidylcholine at GC|npSG-EC. Scan initiated after immersion of the electrode for **a** 5 min and **b** 60 min. Electrolyte, 0.1 M phosphate buffer at pH 7.2; v, 50 mV s^{-1}. At GC coated in the absence of PAMAM, reductions of $Fe(CN)_6^{3-}$ and $Ru(NH_3)_6^{3+}$ were not observed

absence of bovine serum albumin (BSA) at GC, GC|npSG, and GC|npSG-EC electrodes. The influence of BSA on i_{pc} is summarized in Table 2. The decrease of i_{pc} in the presence of 0.2% BSA was 29%, 35%, and 2%, respectively, when the voltammetric scan was initiated 5 min after immersion of the electrode. The data suggest that the BSA neither penetrates the pores of the film nor adsorbs significantly to the end-capped sol-gel. In this regard, the 2% decrease is within the reproducibility of the current measurements. A related concern is the influence of time of exposure of the modified electrode to a macromolecule-containing solution on the voltammetric behavior. Here, a phospholipid, phosphatidylcholine (PC), was used as the test interferent. The voltammetry of $Fe(CN)_6^{3-}$ at GC|npSG-EC in the presence of 0.5 mM PC is shown in Fig. 7. The i_{pc} values after immersion for 5 and 60 min in 0.5 mM PC, 3.66 and 3.65 μA, respectively, are statistically identical. In turn, these currents agree to the value obtained in a blank experiment (same conditions except no PC present), which

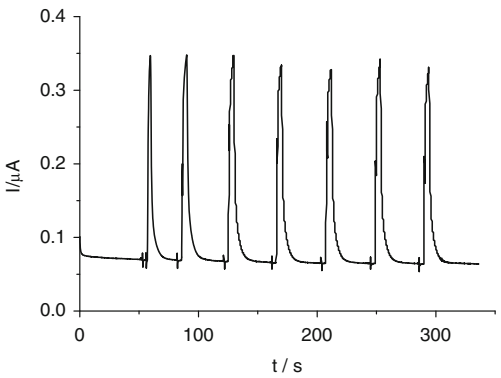

Fig. 8 Flow injection amperometry of 2.0 μM bromate at a GC|APTES-Rh_2PMo_{11} surface within a GC|npSG-EC electrode. Flow rate, 1.0 mL min^{-1}; carrier solution, 0.1 M H_2SO_4; injection volume, 100 μL; applied potential, −0.1 V vs. Ag|AgCl

gave an i_{pc} of 3.67 μA. At GC under the same conditions, the PC decreases i_{pc} by 16% with a 5-min exposure.

The above results demonstrate that the nanoporous, end-capped sol-gel film protects the electrode from passivation by adsorption of proteins and eliminates the influence of the charged sites of silica on the voltammetry of ionic species. In addition, the hypothesized structure in Fig. 1 increased the stability of electrochemical catalysts immobilized in the pores. This point was illustrated by a study where gold nanoparticles that were surface-modified with dirhodium-substituted phosphomolybdic acid (AuNP-Rh_2PMo_{11}), which we have described previously [35], was the catalyst. Adsorption of AuNP-Rh_2PMo_{11} to GC was too weak for long term stability, so it is attached by first modifying GC with aminopropyltrimethoxysilane (APTES) by immersion of GC|npSG-EC in 0.06 M APTES in methanol for 60 min. An infrared spectrum did not show the presence of APTES on the npSG-EC, which is in contrast to the spectrum obtained when GC|npSG was reacted under the same conditions. However, electrochemical evidence of APTES at the GC surface within the modified electrode was obtained. The GC|npSG-EC was placed in an acidic (0.05 M H_2SO_4) solution of AuNP-Rh_2PMo_{11} for 12 h. In contrast to an experiment in the absence of APTES, the characteristic voltammogram for the phosphomolybdate groups was observed. That the APTES was present in GC|npSG-EC but not on the sol-gel phase is evidence that the model in Fig. 1, which has GC exposed at the base of the pore, is valid. In the absence of npSG-EC, the electrode (GC|APTES, AuNP-Rh_2PMo_{11}) is not stable in a flow system; however, the catalyst is stable for at least 4 weeks when it is electrostatically attached to the GC|APTES in the pore structure of npSG-EC. A typical set of replicate flow-injection amperometry curves for the reduction of bromate is shown in Fig. 8. The linear dynamic range is 0.2–10 μM bromate. The detection limit, calculated as the concentration that gives a signal three times the standard deviation of a set of five blank injections, is 30 nM bromate.

Conclusions

When sol-gel films on electrodes are deposited from tetraethoxysilane by a process in which the proton catalyst is electrochemically generated, the reduction of ionic species such as $Fe(CN)_6^{3-}$ and $Ru(NH_3)_6^{3+}$ at this modified electrode is not observed. Inclusion of generation-4 poly (amidoamine) dendrimer in the precursor solution causes the formation of 10±5 nm pores. This process is proposed to occur by adsorption of PAMAM to the electrode, which blocks the electrochemically assisted formation of sol-gel at these sites. Removal of the dendrimer is accomplished with a low-temperature gas plasma. Consistent with literature studies of other structures of sol-gel modified electrodes, the presence of a negative surface charge at pH>2 decreases the voltammetric current for the reduction of $Fe(CN)_6^{3-}$ and increases it for the reduction of $Ru(NH_3)_6^{3+}$ relative to that at the isoelectric point of silica. The influence of charge on the silica also was mitigated by using a high ionic-strength electrolyte (2 M KCl), which causes a breakdown of the Donnan Exclusion Principle. Infrared spectroscopy provides evidence that silanization of the sol-gel converts the hydroxyl to alkyl sites, and SEM imaging shows that this procedure does not damage the film structure, even after removal of the PAMAM with an oxygen plasma. The resulting sol-gel film has an organized pore structure and a neutral surface, which eliminates the influence of pH on the voltammetry of ionic species. Attempts to fabricate an analogous electrode by using an organically modified silane as the precursor failed because the oxygen plasma treatment collapsed the ormosil film structure. The resulting electrode in this study yielded pH-independent voltammetry of charged ions over a wide range and size-excluded selective proteins from reaching the electrode surface. Moreover, the methylated surface eliminated problems related to the adsorption of these proteins to the sol-gel phase. In addition, the pore structure that was achieved blocked the stripping of a catalyst from the underlying electrode under hydrodynamic conditions.

Acknowledgements The work was supported by U.S. National Institutes of Health through grant R15GM087662-01 and by The Institute for the Development and Commercialization of Advanced Sensor Technology (IDCAST) administered by the University of Dayton Research Institute. D. Ranganathan's doctoral research was performed in part at Miami University with support provided by the School of Advanced Studies of the University of Camerino.

References

1. Sittampalam G, Wilson GS (1983) Anal Chem 55:1608
2. Zhang Y, Hu Y, Wilson GS, Moatti-Sirat D, Poitout V, Reach G (1994) Anal Chem 66:1183
3. Wang J, Golden T, Li R (1988) Anal Chem 60:1642
4. Wandstrat MM, Spendel WU, Pacey GE, Cox JA (2007) Electroanalysis 19:139
5. Tanev PT, Pinnavaia TJ (1995) Science 267:865
6. Kanungo M, Deepa PN, Collinson MM (2004) Chem Mater 16:5535
7. Khramov AN, Munos J, Collinson MM (2001) Langmuir 17:8112
8. Shacham R, Avnir D, Mandler D (1999) Adv Mater 11:384
9. Shacham R, Mandler D, Avnir D (2004) Chem Eur J 10:1936
10. Shacham R, Avnir D, Mandler D (2004) J Sol-Gel Sci Technol 31:329
11. Sheffer M, Groysman A, Mandler D (2003) Corros Sci 45:2893
12. Deepa PN, Kanungo M, Claycomb G, Sherwood PMA, Collinson MM (2003) Anal Chem 75:5399
13. Walcarius A, Sibottier E, Etienne M, Ghanbaja J (2007) Nature Mater 6:602

14. Guillemin Y, Etienne M, Aubert E, Walcarius A (2010) J Mater Chem 20:6799
15. Etienne M, Quach A, Grosso D, Nicole L, Sanchez C, Walcarius A (2007) Chem Mater 19:844
16. Hsueh CC, Collinson MM (1997) J Electroanal Chem 420:243
17. Ranganathan D, Zamponi S, Berrettoni M, Mehdi BL, Cox JA (2010) Talanta 82:1149
18. Hierlemann A, Campbell JK, Baker LA, Crooks RM, Ricco AJ (1998) J Am Chem Soc 120:5323
19. Li J, Piehler LT, Qin D, Baker JR, Tomalia DA (2000) Langmuir 16:5613
20. Spatz JP, Mössmer S, Hartmann C, Möller M (2000) Langmuir 16:407
21. Kumar S, Zou S (2009) Langmuir 25:574
22. Evans MB, Dale AD, Little CJ (1980) Chromatographia 12:5
23. Wei H, Collinson MM (1999) Anal Chim Acta 397:113
24. Cox JA, Kulesza PJ (1983) Anal Chim Acta 154:71
25. Kristensen EW, Kuhr WG, Wightman RM (1987) Anal Chem 59:1752
26. Cui X, Zin WC, Cho WJ, Ha CS (2005) Mater Lett 59:2257
27. Zhang B, Zhang Y, White HS (2004) Anal Chem 76:6229
28. Walcarius A, Bessiere J (1997) Electroanalysis 9:707
29. Wu KH, Li MC, Yang CC, Wang GP (2006) J Non-Cryst Solids 352:2897
30. Fattakhova-Rohlfing D, Rathousky J, Rohlfing Y, Bartels O, Wark M (2005) Langmuir 21:11320
31. Anappara AA, Rajeshkumar S, Mukundan P, Warrier PRS, Ghosh S, Warrier KGK (2004) Acta Mater 52:369
32. Karmakar B, De G, Ganguli D (2000) J Non-Cryst Solids 272:119
33. De G, Karmakar B, Ganguli D (2000) J Mater Chem 10:2289
34. Zhang X, Wu Y, He S, Yang D (2007) Surf Coat Technol 201:6051
35. Wiaderek KM, Cox JA (2011) Electrochim Acta 56:3537